



A chemical dynamics study on the gas phase formation of thioformaldehyde (H₂CS) and its thiohydroxycarbene isomer (HCSH)

Srinivas Doddipatla^a, Chao He^a, Ralf I. Kaiser^{a,1}, Yuheng Luo^a, Rui Sun^{a,1}, Galiya R. Galimova^b, Alexander M. Mebel^{b,1}, and Tom J. Millar^{c,1}

^aDepartment of Chemistry, University of Hawai'i at Mānoa, Honolulu, HI 96822; ^bDepartment of Chemistry and Biochemistry, Florida International University, Miami, FL 33199; and ^cSchool of Mathematics and Physics, Queen's University Belfast, Belfast BT7 1NN, Northern Ireland, United Kingdom

Edited by Stephen J. Benkovic, The Pennsylvania State University, University Park, PA, and approved August 4, 2020 (received for review March 13, 2020)

Complex organosulfur molecules are ubiquitous in interstellar molecular clouds, but their fundamental formation mechanisms have remained largely elusive. These processes are of critical importance in initiating a series of elementary chemical reactions, leading eventually to organosulfur molecules—among them potential precursors to iron-sulfide grains and to astrobiologically important molecules, such as the amino acid cysteine. Here, we reveal through laboratory experiments, electronic-structure theory, quasi-classical trajectory studies, and astrochemical modeling that the organosulfur chemistry can be initiated in star-forming regions via the elementary gas-phase reaction of methylidyne radicals with hydrogen sulfide, leading to thioformaldehyde (H₂CS) and its thiohydroxycarbene isomer (HCSH). The facile route to two of the simplest organosulfur molecules via a single-collision event affords persuasive evidence for a likely source of organosulfur molecules in star-forming regions. These fundamental reaction mechanisms are valuable to facilitate an understanding of the origin and evolution of the molecular universe and, in particular, of sulfur in our Galaxy.

reaction dynamics | reactive intermediates | organosulfur molecules | astrochemistry | molecular beams

For nearly half a century, star-forming regions like Sagittarius B2 (Sgr B2) and the Orion Molecular Cloud Complex have been recognized as molecular factories and natural laboratories for advancing our fundamental understanding of the elementary processes directing the synthesis of complex molecules in the interstellar medium (ISM) through astronomical observations coupled with laboratory experiments and astrochemical modeling (1–10). However, with more than 200 molecules—23 of which contain sulfur—as complex as the sugar-related glycolaldehyde (HCOCH₂OH) (11–14) and fullerenes (C₆₀ and C₇₀) (15, 16) detected in interstellar and circumstellar environments, these models have as yet been unsuccessful to account for the occurrence of ubiquitous sulfur-bearing molecules predicting fractional abundances of species like carbonyl monosulfide (CS), thioformaldehyde (H₂CS), and thiomethanol (CH₃SH), falling short by up to two orders of magnitude compared to astronomical observations (Fig. 1) (17, 18). Consequently, although models predict that sulfur-bearing molecules—among them potential precursors to iron-sulfide grains (19) and to astrobiologically important molecules such as the amino acid cysteine—should be in molecular form, observations reveal gas-phase abundances of sulfur-bearing molecules of only up to 1.0% at most. Therefore, the formation routes to sulfur-bearing molecules in the ISM and the chemical reactions involved in coupling the carbon and sulfur chemistries are essentially unknown to date (20).

Contemporary astrochemical models of massive star-formation regions adopt a two-phase model, with the sulfur chemistry initiated by the collapsing cloud and depletion of up to 95% of the atomic and molecular-bound sulfur onto the grain surfaces (21). Surface hydrogenation, along with energetic processing by ultraviolet photons and galactic cosmic rays, has been proposed to convert the hydrogen sulfide (H₂S) reservoir at least partially to

sulfur dioxide (SO₂) (21) and sulfur (S₈) (22). The second phase commences with the formation of the central protostars. Temperatures increase up to 300 K, and sublimation of the (sulfur-bearing) molecules from the grains takes over (20). The subsequent gas-phase chemistry exploits complex reaction networks of ion–molecule and neutral–neutral reactions (17) with models postulating that the very first sulfur–carbon bonds are formed via reactions involving methyl radicals (CH₃) and carbene (CH₂) with atomic sulfur (S) leading to carbonyl monosulfide and thioformaldehyde, respectively (18). Dissociative electron recombination with sulfur-bearing ions (H₃CS⁺ and CH₃SH₂⁺)—hypothesized to be formed via multifaceted chains of ion–molecule reactions—has also been conjectured to form the simplest prototype of a closed shell organosulfur molecule: thioformaldehyde. However, the validity of these gas-phase processes has neither been confirmed experimentally nor computationally, although the elucidation of these elementary reactions is critical to untangle the fundamental pathways that initiate and drive the hitherto poorly constrained sulfur chemistry in deep space.

To fill this gap, we present a combined crossed molecular beam, high-level ab initio, quasi-classical trajectory (QCT) study, and astrochemical modeling on the formation of thioformaldehyde along with its thiohydroxycarbene isomer (HCSH) in the gas phase and explore their role on the chemistry of massive star-forming

Significance

Since the detection of carbonyl monosulfide (CS) in star-forming regions, about 200 molecules as complex as fullerenes have been detected in interstellar and circumstellar environments, but the formation routes to organosulfur molecules have remained essentially elusive. Exploiting thioformaldehyde (H₂CS) and its thiohydroxycarbene isomer (HCSH), we deliver compelling testimony via laboratory experiments, electronic-structure theory, astrochemical modeling, and quasi-classical trajectory studies that these organosulfur species can be efficiently formed in star-forming regions such as Sagittarius B2 through bimolecular reactions involving hydrogen sulfide and methylidyne radicals. These elementary mechanisms are of fundamental importance to aid our understanding of how carbon and sulfur chemistries are connected in deep space, thus expanding our view on the sulfur cycle in the Galaxy.

Author contributions: R.I.K. designed research; S.D., C.H., Y.L., R.S., G.R.G., A.M.M., and T.J.M. performed research; S.D., R.I.K., Y.L., R.S., G.R.G., A.M.M., and T.J.M. analyzed data; and S.D., R.I.K., R.S., A.M.M., and T.J.M. wrote the paper.

The authors declare no competing interest.

This article is a PNAS Direct Submission.

Published under the PNAS license.

¹To whom correspondence may be addressed. Email: ralfk@hawaii.edu, ruisun@hawaii.edu, mebel@fiu.edu, or Tom.Millar@qub.ac.uk.

This article contains supporting information online at <https://www.pnas.org/lookup/suppl/doi:10.1073/pnas.2004881117/-DCSupplemental>.

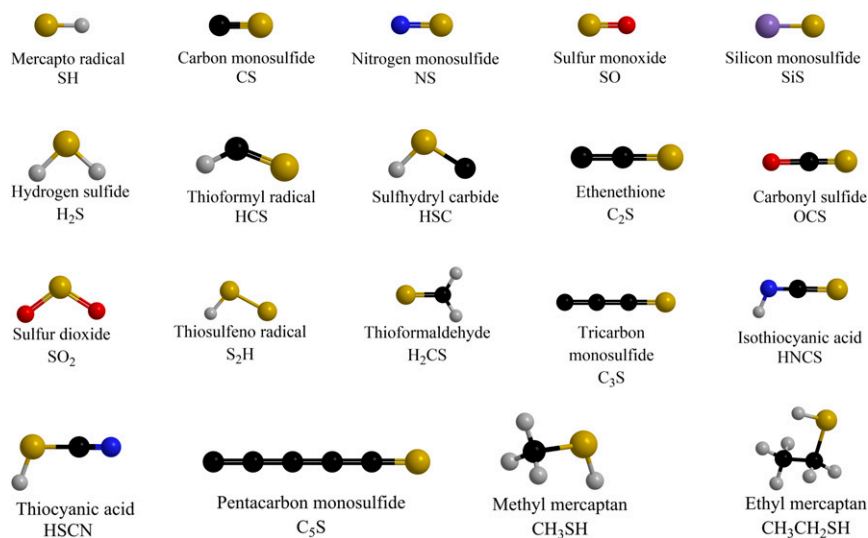
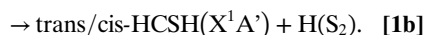
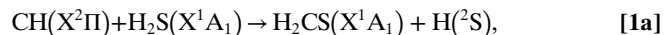


Fig. 1. Neutral sulfur-bearing molecules detected in the ISM. In addition, four molecular ions (SH^+ , NS^+ , SO^+ , and HCS^+) were also detected in interstellar clouds.

regions such as Orion KL and Sgr B2. The reaction of ground-state methylidyne radicals (CH) with hydrogen sulfide was investigated under single-collision conditions revealing the preparation of distinct organosulfur isomers: thioformaldehyde and thiohydroxycarbene (HCSH) (reaction 1). This system represents the prototype reaction of the simplest closed shell hydride of sulfur–hydrogen sulfide, as detected with fractional abundances of up to 10^{-7} in star-forming regions (23, 24)—with the simplest benchmark of an organic radical–methylidyne (CH) generated through photolysis of methane (CH_4) (25)—to prepare key organosulfur molecules via a single-collision event through the coupling of the sulfur and carbon chemistries in star-forming regions. Our investigations also provide dynamical information on the elementary steps to both thioformaldehyde and thiohydroxycarbene isomers. Since the laboratory data strongly depend on the structures of the initially formed collision complexes, along with the products of the reaction, we first calculated the geometries of energetically accessible reaction intermediates and products and identified the transition states connecting them, and then compared our crossed-beam data and experimental dynamics with those arising from OCT studies, eventually shedding light on a key elementary reaction initiating the previously undetected organosulfur chemistry in star-forming regions.



Results and Discussion

Crossed Molecular Beams Studies—Laboratory Frame. Reactive scattering experiments were conducted, exploiting a crossed molecular beam machine by intersecting supersonic beams of electronically ground-state methylidyne (CH ; $X^2\Pi$) and D1-methylidyne radicals (CD ; $X^2\Pi$) with hydrogen sulfide (H_2S ; X^1A_1) and deuterium sulfide (D_2S ; X^1A_1) perpendicularly at collision energies of 19 kJ mol^{-1} under single-collision conditions in the gas phase (*Materials and Methods* and *SI Appendix*, Table S1). The neutral reaction products were ionized via electron impact at 80 eV within a triply differentially pumped quadrupole mass-spectrometric detector and then mass- and velocity-analyzed to record time-of-flight (TOF) spectra of the ionized products at distinct laboratory angles. In the methylidyne

(CH; 13 atomic mass units [amu])–hydrogen sulfide system (H_2^{34}S and H_2^{32}S , 36 and 34 amu), reactive scattering signal was observed at mass-to-charge ratio (m/z) 46 ($\text{H}_2\text{C}^{32}\text{S}^+$) and 45 (HC^{32}S^+) with an intensity ratio of 0.51 ± 0.25 . Signal at m/z 47 ($\text{H}_2^{13}\text{C}^{32}\text{S}^+$) and 48 ($\text{H}_2\text{C}^{34}\text{S}^+$) was too weak to be monitored; this is in line with the low natural abundances of ^{13}C and ^{34}S at levels of 1.1% and 4.2%, along with extended data-accumulation times of up to 21 h (2×10^6 TOF spectra) per angle (Fig. 2). The TOF spectra at m/z 46 and 45 were superimposable after scaling, suggesting that signal at m/z 45 originated from dissociative electron-impact ionization of the parent molecule (H_2CS ; 46 amu) in the ionizer. Therefore, the laboratory data alone provide conclusive evidence on the formation of a reaction product with the chemical formula H_2CS (46 amu) plus atomic hydrogen (1 amu) formed via the reaction of the methylidyne radical (13 amu) with hydrogen sulfide (34 amu) via a single-collision event of two neutral reactants (reaction 1); within our signal-to-noise, no molecular hydrogen-loss pathway could be detected. Fig. 2 depicts the laboratory angular distribution and selected TOF spectra recorded at m/z 46 ($\text{H}_2\text{C}^{32}\text{S}^+$; hereafter, H_2CS^+), which could be fitted with a single channel arising from the methylidyne and hydrogen sulfide reactants. The laboratory angular distribution was relatively broad and spread over at least 45° within the scattering plane; the nearly forward–backward symmetry around the center-of-mass (CM) angle of 48.9° suggests indirect reaction dynamics involving the formation of H_3CS complex(es).

Having established that in the reaction of ground-state methylidyne radicals with hydrogen sulfide, the atomic hydrogen-loss channel results in the formation of H_2CS isomer(s) (reaction 1a), we then elucidated to what extent the hydrogen atom is lost from the methylidyne radical, from the hydrogen sulfide reactant, or from both. Therefore, we conducted the crossed-beam reactions of methylidyne (CH ; $X^2\Pi$; 13 amu) with deuterium sulfide (D_2S ; X^1A_1 ; 36 amu) and of D1-methylidyne (CD ; $X^2\Pi$; 14 amu) with hydrogen sulfide (H_2S ; X^1A_1 ; 34 amu) to explore the position of the atomic hydrogen loss. Any ejection of a loss of a hydrogen atom should result in reactive scattering signal at m/z 48 (D_2CS^+) and m/z 47 (HDCS^+), respectively (reactions 2a and 3a). In the CD/ H_2S system, reactive scattering signal was observed at m/z 47 and 46 at a ratio of 0.57 ± 0.31 (*SI Appendix*, Fig. S1). Signal at m/z 47 unequivocally demonstrated the elimination of atomic hydrogen and formation of HDCS isomer(s) (reaction 3a). Ion counts at m/z 46 could arise from an atomic deuterium-loss pathway (reaction 3b) and/or dissociative electron-impact ionization of the neutral

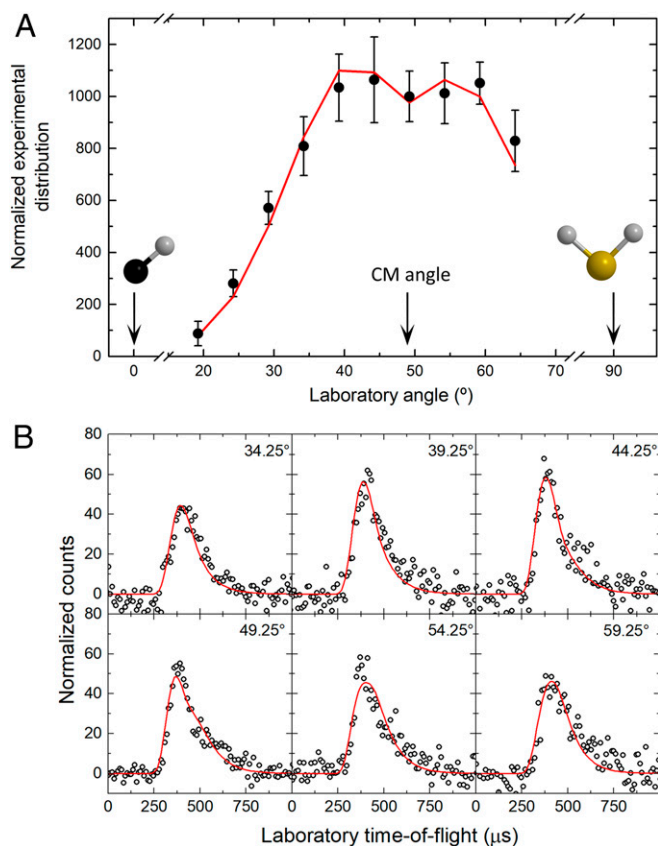
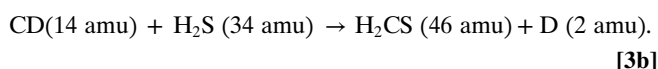
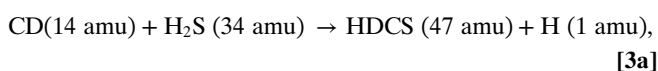
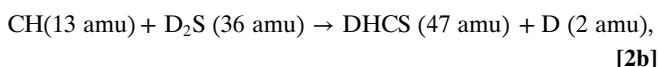
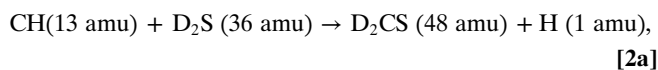


Fig. 2. (A) Laboratory angular distributions of the products recorded at m/z 46 (H_2CS^+) for the reactions of hydrogen sulfide and methylidyne radicals. The filled circles represent the experimental data, C.M. designates the CM angle, the error bars represent the 1σ SD, and red solid lines represent the overall fit. (B) Selected TOF spectra are presented; open circles depict the experimental data and the solid lines the fit.

HDCS. Considering the CH/ D_2S system, only weak ion counts were detected at m/z 48 (D_2CS^+) (reaction **2a**); signal at m/z 47 (reaction **2b**) was of similar intensity as in the CD/ H_2S system and

can only be explained via atomic deuterium loss leading to the formation of DHCS **47** (reaction **2b**), but not from dissociative electron-impact ionization of D_2CS . Note that the ratio of the ion counts of m/z 48 vs. 47 is only 0.08 ± 0.02 ; this finding suggests that signal at m/z 48 not only originates from DH^{13}CS , but also from atomic hydrogen loss. In summary, the isotopic substitution experiments reveal that the ejected atomic hydrogen/deuterium predominantly originates from the (deuterated) hydrogen sulfide reactant and to a smaller fraction from the (deuterated) methylidyne radical.



Crossed Molecular Beams Studies—CM Frame. The analysis of the raw data revealed compelling evidence that, for the reaction of ground-state methylidyne radicals with hydrogen sulfide, a molecule with the chemical formulae H_2CS is formed via atomic hydrogen elimination, with the hydrogen originating predominantly from the hydrogen sulfide reactant. To gain information on the underlying reaction dynamics, we transformed the experimental data from the laboratory to the CM reference frame (26, 27); this process yielded the CM translational energy-flux distribution $P(E_T)$ and the CM angular-flux distribution $T(\theta)$ (Fig. 3). Best fits of the laboratory data could be accomplished with a single-channel fit yielding products with a mass combination of 46 amu (H_2CS) and 1 amu (H). The $P(E_T)$ supported in the identification of the product isomer(s). For reaction products formed without internal excitation, the high-energy cutoff of $275 \pm 25 \text{ kJ}\cdot\text{mol}^{-1}$ represents the sum of the absolute value of the reaction exoergic plus the collision energy E_c ($18.9 \pm 0.4 \text{ kJ}\cdot\text{mol}^{-1}$). Based on energy conservation, a subtraction of the collision energy suggests that the

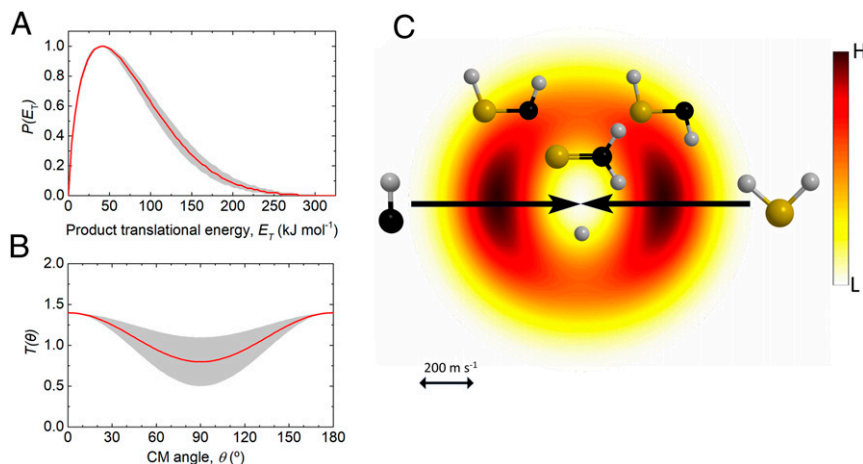


Fig. 3. CM translational energy distribution $P(E_T)$ (A) and angular distribution $T(\theta)$ (B) along with the associated flux contour map (C) leading to the formation of thioformaldehyde and *trans/cis*-thiohydroxycarbene (HCSH). Shaded areas indicate the error limits of the best fits, accounting for the uncertainties of the laboratory angular distribution and TOF spectra, with the red solid lines defining the best-fit functions. The flux contour map represents the flux intensity of the reactive scattering products as a function of the CM scattering angle (θ) and product velocity (u). The color bar indicates the flux gradient from high (H) intensity to low (L) intensity. Atoms are color-coded as follows: sulfur (yellow); carbon (black); and hydrogen (gray).

reaction is highly exoergic with an energy of $-256 \pm 25 \text{ kJ}\cdot\text{mol}^{-1}$. The $P(E_T)$ peaks away from zero translational energy at around 30 to 50 $\text{kJ}\cdot\text{mol}^{-1}$; this finding proposes the existence of a tight exit transition state for the decomposition of the H_3CS complex(es), accompanied by a significant electron-density rearrangement upon the atomic hydrogen loss (28). Finally, the $T(\theta)$ is forward-backward symmetric and extends over the complete angular range from 0° to 180° with a forward-backward symmetry. These findings propose indirect scattering dynamics via long-lived H_3CS intermediates whose lifetimes are longer than, or at least competitive with, their rotation periods. The distribution minimum at 90° suggests geometrical constraints with the hydrogen atom emitted perpendicularly to the total angular momentum vector almost within the rotational plane of the decomposing H_3CS complex(es) (28, 29).

Electronic Structure and Dynamics Calculations. With the identification of the H_2CS isomer(s) as the product of the bimolecular gas-phase reaction of the methylidyne radical with hydrogen sulfide along with the preferential emission of the hydrogen atom from the hydrogen sulfide reactant, it is our goal to elucidate the underlying chemical dynamics and reaction mechanism(s). This is achieved by combining our experimental findings with electronic structure and molecular-dynamics calculations. Reactants, products, intermediates, and transition-state structures relevant to the reaction of ground-state methylidyne radicals with hydrogen sulfide were characterized and compiled in the potential energy surface (Fig. 4 and *SI Appendix*, Fig. S2). These calculations predicted the existence of eight reaction channels. The *atomic hydrogen* loss leads to the thermodynamically most stable thioformaldehyde isomer (H_2CS , X^1A_1 , **p1**), which is energetically favorable by 183 $\text{kJ}\cdot\text{mol}^{-1}$ compared to its *trans* thiohydroxycarbene structure (HCSH , X^1A' , **p2trans**); owing to the repulsion of both hydrogen atoms, the *cis* thiohydroxycarbene species (HCSH , X^1A' , **p2cis**) is destabilized by 5 $\text{kJ}\cdot\text{mol}^{-1}$. These energy differences are in excellent agreement with a previous computational investigation of the thioformaldehyde (**p1**)–*trans/cis* thiohydroxycarbene (**p2trans/cis**) isomer pair of 183 and 4 $\text{kJ}\cdot\text{mol}^{-1}$, respectively (30). Sato et al. (31) and Guest and coworkers (32) predicted *trans* thiohydroxycarbene (**p2trans**) to be less stable by 186 and 198 $\text{kJ}\cdot\text{mol}^{-1}$ compared to thioformaldehyde (**p1**). The first excited triplet state of thiohydroxycarbene (HCSH , a^3A' , **p2trip**) lies 33 $\text{kJ}\cdot\text{mol}^{-1}$ above the energy of the separated reactants and, hence, is energetically not accessible, considering a collision energy of 18.9 $\text{kJ}\cdot\text{mol}^{-1}$ in the present experiments. The computed singlet–triplet gap of thiohydroxycarbene of 78 $\text{kJ}\cdot\text{mol}^{-1}$ agrees well with the prediction of Schreiner and coworkers (33) of about 71 $\text{kJ}\cdot\text{mol}^{-1}$. The *molecular hydrogen* loss is accompanied by the formation of the thioformyl (HCS , X^2A' , **p3**) and isothioformyl (HSC ,

X^2A' , **p4**) radicals with overall reaction exoergicities of 283 and 121 $\text{kJ}\cdot\text{mol}^{-1}$ with respect to the separated reactants. The energy difference of both isomers of 162 $\text{kJ}\cdot\text{mol}^{-1}$ is in line with previous calculations by Ochsenfeld, Head-Gordon, and coworkers (30) revealing a thioformyl isomer, which lies 166 $\text{kJ}\cdot\text{mol}^{-1}$ lower in energy than isothioformyl. Finally, two *carbon–sulfur bond-cleavage* channels lead to ground-state atomic sulfur (S , 3P) plus the methyl radical (CH_3 , X^2A_2'' , **p5**) and thiohydroxyl (HS , $X^2\Pi$) plus triplet carbene (CH_2 , X^3B_2) (**p6**); the direct hydrogen-abstraction channel forming thiohydroxyl plus carbene has to pass a transition state located 25 $\text{kJ}\cdot\text{mol}^{-1}$ above the separated reactants; hence, this pathway is closed under our experimental conditions at collision energies of 18.9 $\text{kJ}\cdot\text{mol}^{-1}$.

Our computations revealed further the existence of three doublet reaction intermediates (**i1**–**i3**). The reaction of methylidyne with hydrogen sulfide can be initiated by the barrierless *addition* to the sulfur atom and/or *insertion* into the sulfur–hydrogen bond, leading to collision complexes **i1** and **i2**, respectively. Both intermediates can be interconverted through a transition state located about 50 $\text{kJ}\cdot\text{mol}^{-1}$ below the energy of the separated reactants. The thiohydroxymethyl radical intermediate **i2** may undergo a hydrogen shift from the sulfur to the carbon atom, yielding the thiomethoxy radical (**i3**). The thiohydroxymethyl–thiomethoxy system is isovalent to the hydroxymethyl–methoxy radical pair. Among these three intermediates, **i2** and **i3** can both eject a hydrogen atom forming thioformaldehyde (**p1**). Four reaction pathways may connect to singlet *cis/trans* thiohydroxycarbene (HCSH) (**i1**→**p2trans**/**p2cis**; **i2**→**p2trans**/**p2cis**). Interestingly, besides the atomic hydrogen loss, our computations also located two molecular hydrogen-loss pathways leading from intermediates **i3** and **i2** to thioformyl (HCS , X^2A' , **p3**) and isothioformyl (HSC , X^2A' , **p4**) via tight exit transition states. The aforementioned intermediates are also linked to carbon–sulfur bond-rupture channels forming atomic sulfur (S , 3P) plus methyl (CH_3 , X^2A_2'' , **p5**) and thiohydroxyl (HS , $X^2\Pi$) plus triplet carbene (CH_2 , X^3B_2 , **p6**).

An association of these computations with our experimental data leads to interesting findings. A comparison of these data with the experimental reaction energy for the atomic hydrogen-loss pathway of $-256 \pm 25 \text{ kJ}\cdot\text{mol}^{-1}$ suggests an excellent correlation with the computed reaction exoergicities of $233 \pm 10 \text{ kJ}\cdot\text{mol}^{-1}$, leading at least to thioformaldehyde (H_2CS , X^1A_1 , **p1**) via indirect scattering dynamics through the involvement of CH_3S intermediate(s) **i2** and/or **i3** holding a lifetime longer than the (ir) rotational period(s). This reveals that thioformaldehyde can be formed in the gas phase as a result of a reaction between two neutral species under controlled experimental conditions via a single-collision event. It is important to highlight that the formation of the less

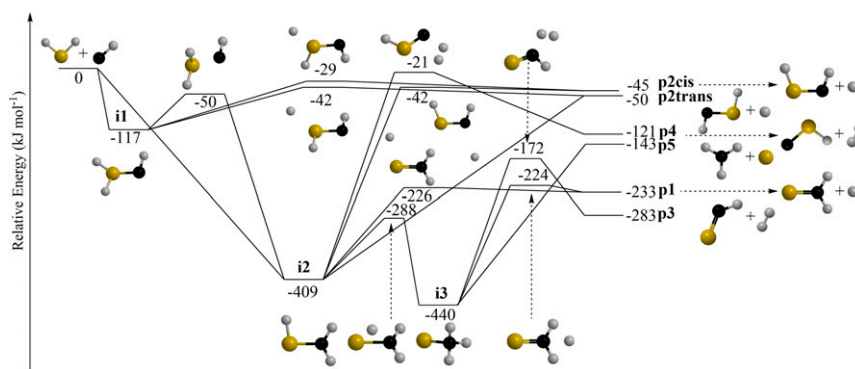


Fig. 4. Potential energy surface for the reactions of hydrogen sulfide with methylidyne (CH). Relative energies calculated at the CCSD(T)-F12/cc-pVQZ-f12//B2PLYPD3/cc-pVTZ + ZPE(B2PLYPD3/cc-pVTZ) level of theory are given in units of $\text{kJ}\cdot\text{mol}^{-1}$. The potential energy surface is simplified by removing barriers and reaction products above the 18.9 $\text{kJ}\cdot\text{mol}^{-1}$ collision energy (*SI Appendix*, Fig. S2). Atoms are color-coded as follows: sulfur (yellow); carbon (black); and hydrogen (gray).

stable singlet *cis/trans* thiohydroxycarbene isomers (HCSH, **p2cis/trans**) cannot be ruled out at the present stage, since their contribution can be “hidden” in the low-energy part of the CM translational energy distribution. Further, the computationally predicted molecular hydrogen-loss channel could not be verified experimentally; this suggests that the molecular hydrogen-loss pathway(s) only holds a minor fraction at a level of some percent within the detection limit of our experimental setup. Finally, the accessible reaction channel opening up from carbon–sulfur bond cleavage (**p5** and **p6**) cannot be probed in our setup because the *m/z* values of the ionized products would overlap with fragment ions of the reactants along with their isotopically labeled counterparts.

These open queries call for QCT calculations (34, 35), thus bridging the dynamics experiments with the theoretical understanding of the methylidyne–hydrogen sulfide system (*SI Appendix*). In QCT, the reactants are propagated by solving classical equations of motion with the accelerations calculated with an ab initio method on-the-fly. It is important to note that millions of ab initio calculations are involved in QCT; therefore B3LYP/aug-cc-pVDZ (36, 37) was employed for its balance between computation cost, accuracy, and trajectory stability (*SI Appendix*). Overall, 500 trajectories were sampled at collision energies of 18 kJ mol^{-1} by systematically varying the impact parameter from 100 to 500 pm in steps of 100 pm; since no reactions were observed at impact parameters of 500 pm, simulations with larger impact parameters were not conducted (*SI Appendix*, Table S3). These trajectory studies revealed stimulating results and provided explicit evidence on two distinct entrance channels via methylidyne addition to the sulfur atom of hydrogen sulfide and methylidyne insertion into the sulfur–hydrogen bond, yielding intermediates **i1** and **i2**, respectively (Fig. 5 and *Movies S1–S7*). Considering the larger cone of acceptance of the non-bonding electron pairs of sulfur, nearly two out of three trajectories led to addition ($63 \pm 3\%$), while only one out of three trajectories proceeded via insertion (*SI Appendix*, Table S4; $37 \pm 3\%$). Considering the barrier heights, collision complex **i1** isomerizes to **i2** via hydrogen shift from the sulfur to the carbon atom and may also eject atomic hydrogen-forming *cis/trans* thiohydroxycarbene isomers (HCSH; **p2**) with fractions of $55 \pm 4\%$ (isomerization) and $45 \pm 4\%$ (hydrogen-atom loss) averaged over all impact parameters. The thiohydroxymethyl intermediate **i2** may eliminate atomic hydrogen to yield thioformaldehyde (H_2CS ; **p1**) ($18 \pm 4\%$) and, to a minor amount, *cis/trans* thiohydroxycarbene isomers (HCSH; **p2**) ($6 \pm 2\%$); considering the barrier of only 121 kJ mol^{-1} , the hydrogen-atom migration from the sulfur to the carbon atom leading to the thiomethoxy radical **i3** dominates ($75 \pm 4\%$). It is important to highlight that the trajectory calculations reveal the formation of thioformaldehyde (H_2CS ; **p1**) and of singlet *cis/trans* thiohydroxycarbene (HCSH; **p2**). Considering the atomic hydrogen loss, $70 \pm 3\%$ of the trajectories lead to thioformaldehyde (H_2CS ; **p1**) and $30 \pm 3\%$ to *cis/trans* thiohydroxycarbene isomers (HCSH; **p2**) with the reaction sequences **i1** → **i2** → **p1** + **H** and **i1** → **p2** + **H** dominating the formation of thioformaldehyde (H_2CS ; **p1**) and of singlet *cis/trans* thiohydroxycarbene (HCSH; **p2**), respectively (Fig. 5). Interestingly, these results closely match statistical branching ratios obtained by RRKM (Rice–Ramsperger–Kassel–Marcus) calculations at the collision energy of 19 kJ mol^{-1} , 66% and 32% for **p1** and **p2trans/p2cis**, respectively (*SI Appendix*, Table S6), assuming the $63\%/37\%$ initial formation of **i1/i2** in the entrance channel, as evaluated by the trajectory calculations. The trajectory calculations also allowed us “tagging” the hydrogen atoms at the methylidyne and hydrogen sulfide reactants. Overall, the hydrogen atom was emitted preferentially from the hydrogen sulfide reactant ($86 \pm 2\%$) compared to the methylidyne radical ($14 \pm 2\%$) (*SI Appendix*, Table S5). Finally, we also explored the potential importance of molecular hydrogen loss (**p3/p4**) and carbon–sulfur bond-cleavage processes (**p5** and **p6**) compared to atomic hydrogen loss. The overall product-branching ratios are: $77 \pm 3\%$ for the atomic hydrogen loss, $7 \pm 1\%$ for the molecular

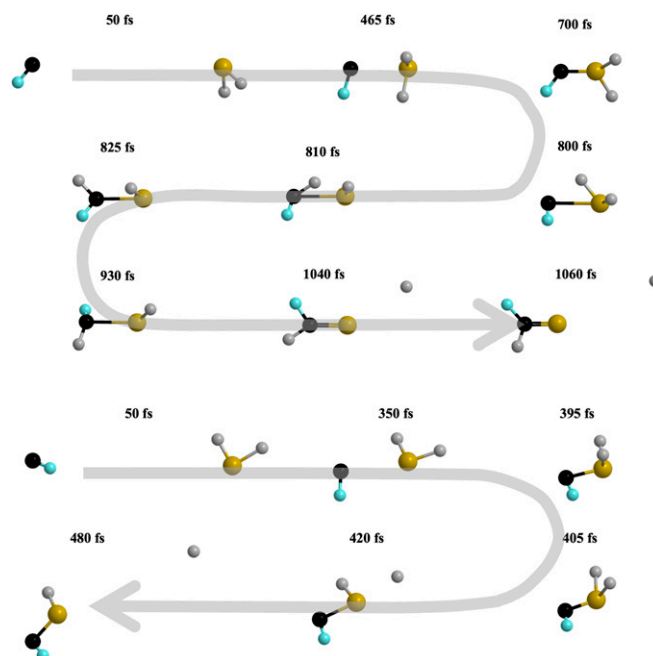


Fig. 5. Snapshots of two representative trajectories from QCT simulations leading to thioformaldehyde and thiohydroxycarbene. The *Upper* snapshots show a trajectory following **i1** → **i2** → **p1** + **H**, and the *Lower* snapshots show a trajectory following **i1** → **p2** + **H**. The hydrogen atom initially belonging to the methylidyne radical is colored with light blue. The movies can be accessed as *Movies S1* and *S5*.

hydrogen loss, and $15 \pm 2\%$ for the carbon–sulfur bond cleavage (*SI Appendix*, Table S3). These results correlate well with our findings of a dominating hydrogen-loss pathway leading to thioformaldehyde (H_2CS ; **p1**) and singlet *cis/trans* thiohydroxycarbene (HCSH; **p2**) with branching ratios of the molecular hydrogen loss to be too low to be observed in our scattering experiments. Optimized Cartesian coordinates and vibrational frequencies of reactants, intermediates, transition states, and dissociation products are given in *SI Appendix*, Table S7.

Astrochemical Modeling and Implications. Having established the formation of thioformaldehyde (H_2CS ; **p1**) and of singlet *cis/trans* thiohydroxycarbene (HCSH; **p2**) under single-collision conditions in the laboratory along with electronic structure and QCT calculations, we then deliberated on potential astrochemical implications. It is vital to transfer these findings to “real” interstellar environments since experiments conducted under well-defined laboratory conditions can scarcely replicate the chemical complexity of the ISM. Our studies revealed explicitly that the reaction has no entrance barrier, that all barriers involved in the formation of thioformaldehyde and thiohydroxycarbene are well below the energy of the separated reactants, and that the overall reactions to prepare both isomers are exergonic. These results represent crucial requirements for this reaction to be important, not only in low-temperature molecular clouds (10 K) (38), but also in star-forming regions where the newborn stars drive the sublimation of the icy grains at temperatures as high as 300 K (17). The entrance barrier would prohibit these reactions in low-temperature interstellar environments. Consequently, our findings can be universally related to any interstellar environment, such as molecular clouds and also star-forming regions, where ice mantles and, most importantly, sufficient hydrogen sulfide can be removed from grains by sublimation (20) and where adequate concentrations of methylidyne radicals and hydrogen sulfide exist. This conclusion also

gains full support from earlier kinetics studies of the methylidyne–hydrogen sulfide system, revealing high rate constants at 295 to 300 K from 2×10^{-10} to 3×10^{-10} $\text{cm}^3 \cdot \text{s}^{-1}$ (39). Consequently, barrierless reactions between methylidyne radicals and hydrogen sulfide are very fast, close to the collisional kinetic limit, at astrochemically relevant temperatures.

We performed astrochemical model simulations exploiting a network of gas-phase reactions in the Orion Hot Core utilizing the chemical kinetic data of the University of Manchester Institute of Science and Technology (UMIST) Database for Astrochemistry (40). Chemical and physical parameters for the simulations were extracted from Esplagues et al. (17) and were operated at typical densities of 2×10^7 cm^{-3} at temperatures of 100 to 200 K (40). This reaction network was updated by the additional reactive chemistry of the methylidyne radical with hydrogen sulfide and removing all ion–molecule and neutral–neutral reactions leading to thioformaldehyde, which were not studied experimentally in any laboratory. The hot molecular core (HMC) model starts with an initial fractional abundance of hydrogen sulfide of 2×10^{-6} as sublimed from the grains; this is about 10% of the elemental sulfur. These HMC models resulted in intriguing findings. First, the fractional abundances derived for thioformaldehyde (H_2CS ; **p1**) in the range of the chemical processing of the Hot Core of 10^4 y to a few hundred thousand years are consistent with the astronomical observations defined by the gray bars of $(0.1$ to $4.0) \times 10^{-9}$ (Fig. 6). One should note that, although the chemistry is simulated for up to 10^7 y, HMCs are young objects with ages in the range of 10^4 y to a few hundred thousand years. Second, at ages of less than a few hundred thousand years, the bimolecular reaction of methylidyne with hydrogen sulfide provides the dominating route to thioformaldehyde (H_2CS ; **p1**). Third, since our experiments revealed that thioformaldehyde (H_2CS ; **p1**) and *cis/trans* thiohydroxycarbene (HCSH ; **p2**) are formed simultaneously, we may predict that *cis/trans* thiohydroxycarbene (HCSH ; **p2**) should be present in HMCs, such as the Orion core at fractional abundances of about 0.3 to 0.5 times that of thioformaldehyde (H_2CS ; **p1**). It should be noted that, once formed, thioformaldehyde (H_2CS ; **p1**) cannot isomerize to *trans* thiohydroxycarbene (HCSH ; **p2**), since a barrier of isomerization of $85 \text{ kJ} \cdot \text{mol}^{-1}$ above the energy of the separate reactants separates both isomers (*SI Appendix*).

Conclusions

Our investigations provide a solid foundation on the formation of two of the simplest closed-shell organosulfur molecules—thioformaldehyde (H_2CS ; **p1**) and the previously astronomically unobserved singlet *cis/trans* thiohydroxycarbene (HCSH ; **p2**)—via elementary neutral–neutral reactions. Previous routes have predominantly speculated on the involvement of unstudied and, hence, unconfirmed chains of ion–molecule reactions (18) terminated by dissociative recombination and hypothetical formation of thioformaldehyde (H_2CS ; **p1**). Consequently, our results challenge conventional wisdom that the organosulfur chemistry in star-forming regions is dictated by complex networks of ion–molecule reactions with previous astrochemical models hardly reproducing observed fractional abundances of thioformaldehyde of up to 4×10^{-9} in the Orion Hot Core star-forming region (40). Consequently, the ability of barrierless, exoergic, neutral–neutral reactions between methylidyne and hydrogen sulfide suggests that this elementary reaction might trigger complex chains of elementary reactions, leading to a rich sulfur chemistry in star-forming regions. Combined experimental and computational studies as provided here also represent a template to shed light on the nature of the molecular carriers of the unknown sulfur reservoir in the gas phase (41, 42)—among them perhaps thiohydroxycarbene (HCSH ; **p2**), as detected here—which are critically required to account for the missing sulfur budget in our Galaxy. Structural isomers in particular, such as the thioformaldehyde

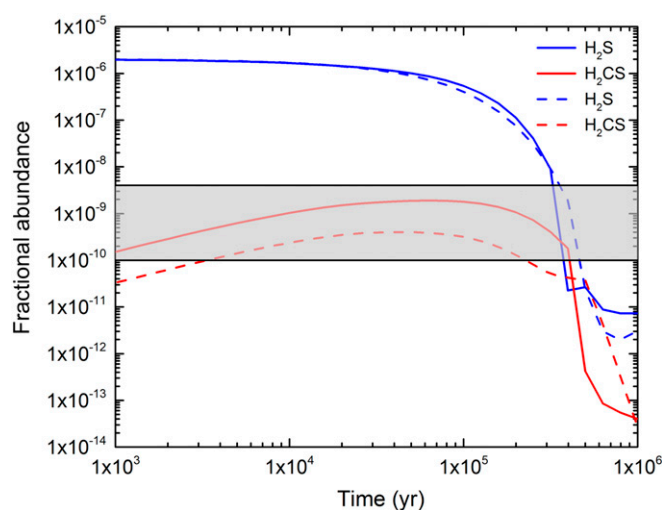


Fig. 6. Time-dependent evolution of the abundances relative to molecular hydrogen of hydrogen sulfide and thioformaldehyde in models of HMCs at a density of $n(\text{H}_2) = 2 \times 10^7$ cm^{-3} and kinetic temperatures of 100 and 200 K. The gray shaded areas show the range of thioformaldehyde fractional abundances derived from observations (23, 40); solid and dashed lines represent temperatures of 100 and 200 K, respectively.

(H_2CS ; **p1**)–thiohydroxycarbene (HCSH ; **p2**) isomer pair, can be exploited as molecular tracers to define the physical and chemical conditions in star-forming regions (23, 43). With thioformaldehyde (H_2CS ; **p1**) residing ubiquitously in star-forming regions and branching ratios of thioformaldehyde to thiohydroxycarbene of typically three to one derived from the present study, fractional abundances of thiohydroxycarbene of up to 10^{-9} with respect to molecular hydrogen are predicted. Consequently, the prospective detection of *trans/cis* thiohydroxycarbene, which have dipole moments of 1.8 and 2.6 Debye, respectively (33), would be invaluable to test future chemical models of the organosulfur chemistry in star-forming regions. In terrestrial laboratories, all previous attempts to detect *trans/cis*-thiohydroxycarbene spectroscopically in the gas phase or in low-temperature matrices were unsuccessful, although Lamberts suggested that thiohydroxycarbene should represent a reactive intermediate in the hydrogenation of carbonyl monosulfide (CS) on interstellar grains (44). The high reactivity, even in low-temperature matrices, might be associated with the molecular structure of thiohydroxycarbene, suggesting that thiohydroxycarbene is not a true carbene, but, rather, a ylide with a negatively charged carbon atom and a positively charged sulfur atom (33). However, the vast regions of space represent a unique natural laboratory on a macroscopic scale and, hence, an unprecedented opportunity to search for highly reactive molecules such as thiohydroxycarbene. With the commission of the Atacama Large Millimeter/Submillimeter Array, the detection of exotic organosulfur molecules, such as thiohydroxycarbene, will intensify. An understanding of these data will rely on critical advances in experimental and computational chemical dynamics as achieved here, thus closing the gap between observational and laboratory data on the extraterrestrial sulfur chemistry that has existed for decades and, hence, changing the way we think about the organosulfur chemistry in the ISM.

Materials and Methods

Experimental. Reactive scattering experiments were carried out under single-collision conditions, as provided in a crossed molecular beam machine (45) by intersecting supersonic beams of electronically ground-state methylidyne (CH ; $X^2\Pi$) and D1-methylidyne radicals (CD ; $X^2\Pi$) with hydrogen sulfide (H_2S ; X^1A_1) and deuterium sulfide (D_2S ; X^1A_1) perpendicularly at collision energies of $19 \text{ kJ} \cdot \text{mol}^{-1}$. A pulsed supersonic beam of methylidyne radicals (CH ; $X^2\Pi$)

was generated by photolysis of bromoform (99%; Sigma-Aldrich Chemistry) at 248 nm (KrF; Coherent) seeded in helium (He; 99.9999%; Gaspro) at backing pressure of 1,672 Torr in the primary source chamber. Defined peak velocities (v_p) and speed ratios (S) chosen by a four-slit chopper wheel rotating at 120 Hz intersected the hydrogen sulfide ($\geq 99\%$; Sigma-Aldrich Chemistry) pulsed beam at a backing pressure of 550 Torr. Methylidyne radicals rotational temperature was determined to be 14 K by laser-induced fluorescence (46). Any reactively scattered neutral products were detected by a rotatable, triply differentially pumped, ultrahigh vacuum chamber (6×10^{-12} Torr) in which neutral products were electron-impact-ionized, then mass-filtered by utilizing a quadrupole mass filter and detected by a Dalry-type TOF detector. The rotatable detector within the plan of both reactant beams allowing the collection of up to 2×10^6 TOF angular-resolved TOF spectra at discrete angles, integrated and normalized them with respect to the intensity at the CM angle yield the laboratory angular distribution. In order to obtain information on scattering dynamics, a forward-convolution routine was employed to convert the laboratory-frame data into the CM frame (26, 27). Considering the reaction has no entrance barrier, a reactive scattering cross-section of an $E_T^{-1/3}$ energy dependence with E_T defining the translational energy within the line-of-center model for entrance barrierless, exoergic reactions was exploited.

QCT Simulation. The QCT simulation propagates the trajectory of the bimolecular collision of hydrogen sulfide and methylidyne radicals by solving the classical equations of motion with energy gradient computed from quantum mechanics. B3LYP with aug-cc-pvdz was selected for the QCT simulation for its moderate computation cost and accuracy in representing the potential energy profile of the reaction (SI Appendix, Table S2). The software employed for the quantum chromodynamics simulation was a combination of a general molecular-dynamics software, VENUS, and a quantum-chemistry software, NWChem (Version 6.3). VENUS generated initial configurations for an ensemble of trajectories and propagated them with potential energy gradients and Hessian calculated from NWChem. To match the condition of the crossed-beam experiments, the vibrational and rotational energy of hydrogen sulfide was generated according to a Boltzmann distribution of 10 K, while the vibration and rotation quantum numbers of methylidyne were approximated as 14 K. The two molecules were separated by 10 Å initially (with orientations chosen randomly) and were set to collide with each

other with a relative translational energy of 18 kJ.mol⁻¹. The timestep of the ab initio molecular dynamics simulation was 0.05 fs and was subject to further reduction until the total energy of the trajectories became stable. The position of the atoms was updated with the velocity Verlet algorithm. The trajectory was halted after it formed a product or went back to the reactant, however long it took. A total of 100 trajectories were sampled at each impact parameter (b), starting from 1.0 Å, with an increment of 1.0 Å, to detect b_{max} , the largest impact parameter of which a trajectory is reactive. The trajectories were weighted with respect to b to ensure that the cross-section of the collision was properly sampled.

Astrochemical Modeling. We modeled those interstellar sources in which hydrogen sulfide is abundant, namely, HMCs, which have typical molecular hydrogen-number densities in the range 10^6 to 10^8 cm⁻³ and kinetic temperatures between 100 and 300 K. Such sources are found in regions of high-mass star formation and contain such large column densities of molecular hydrogen and dust that photo-processing of the gas is unimportant, even though very luminous, young hot stars provide the heating necessary to get to these high temperatures. We calculated the time-dependent chemical kinetic evolution of the hot gas using the full set of reactions and rate coefficients contained in the UMIST Database for Astrochemistry 2012 (47), with additional reactions to describe the formation of silicon dioxide (SiO₂) (48) and, here, thioformaldehyde. As initial conditions for these calculations, molecules were injected into the hot gas from the sublimation of the ice mantles from the grains. The adopted initial abundances were consistent with those observed in ices in cold dark clouds. Abundances relative to molecular hydrogen were extracted from the model and plotted against time.

Data Availability. All data that were generated during the current research are available in the paper and SI Appendix.

ACKNOWLEDGMENTS. The experimental studies were supported by the NSF Award CHE-1360658. The QCT simulations were carried out with high-performance computers from the information technology service from the University of Hawai'i, Manoa, and the Extreme Science and Engineering Discovery Environment. T.J.M. was supported by Science and Technology Facilities Council (UK) Grant ST/P000312/1.

1. A. A. Penzias, P. M. Solomon, R. W. Wilson, K. B. Jefeerts, Interstellar carbon monosulfide. *Astrophys. J.* **168**, L53 (1971).
2. A. Belloche, H. S. P. Müller, R. T. Garrod, K. M. Menten, Exploring molecular complexity with ALMA (EMoCA): Deuterated complex organic molecules in Sagittarius B2(N2). *Astron. Astrophys.* **587**, A91 (2016).
3. A. Schwörner *et al.*, The physical and chemical structure of Sagittarius B2 IV. Converging filaments in the high-mass cluster forming region SgrB2(N). *Astron. Astrophys.* **628**, A6 (2019).
4. A. Fuente, A. Rodríguez-Franco, S. García-Burillo, J. Martín-Pintado, J. H. Black, Observational study of reactive ions and radicals in PDRs. *Astron. Astrophys.* **406**, 899–913 (2003).
5. J. Pety *et al.*, The anatomy of the OrionB giant molecular cloud: A local template for studies of nearby galaxies. *Astron. Astrophys.* **599**, A98 (2017).
6. A. O. H. Olofsson *et al.*, A spectral line survey of Orion KL in the bands 486–492 and 541–577 GHz with the Odin satellite I. The observational data. *Astron. Astrophys.* **476**, 791–806 (2007).
7. T. J. Millar, E. Herbst, Organo-sulphur chemistry in dense interstellar clouds. *Astron. Astrophys.* **231**, 466–472 (1990).
8. P. Caselli, T. I. Hasegawa, R. Herbst, Chemical differentiation between star-forming regions: The Orion Hot Core and Compact Ridge. *Astrophys. J.* **408**, 548–558 (1993).
9. I. R. Cooke, I. R. Sims, Experimental studies of gas-phase reactivity in relation to complex organic molecules in star-forming regions. *ACS Earth Space Chem.* **3**, 1109–1134 (2019).
10. E. Herbst, E. F. van Dishoeck, Complex organic interstellar molecules. *Annu. Rev. Astron. Astrophys.* **47**, 427–480 (2009).
11. J. M. Hollis, F. J. Lovas, P. R. Jewell, Interstellar glycolaldehyde: The first sugar. *Astrophys. J.* **540**, L107–L110 (2000).
12. M. T. Beltran, C. Codella, S. Viti, R. Neri, R. Cesaroni, First detection of glycolaldehyde outside the galactic center. *Astrophys. J.* **690**, L93–L96 (2009).
13. J. K. Jørgensen *et al.*, Detection of the simplest sugar, glycolaldehyde, in a solar-type protostar with ALMA. *Astrophys. J. Lett.* **757**, L4 (2012).
14. H. Calcutt *et al.*, A high-resolution study of complex organic molecules in hot cores. *Mon. Not. R. Astron. Soc.* **443**, 3157–3173 (2014).
15. J. Cami, J. Bernard-Salas, E. Peeters, S. E. Malek, Detection of C₆₀ and C₇₀ in a young planetary nebula. *Science* **329**, 1180–1182 (2010).
16. K. Sellgren *et al.*, C₆₀ in reflection nebulae. *Astrophys. J. Lett.* **722**, L54–L57 (2010).
17. G. B. Espugues, S. Viti, J. R. Goicoechea, J. Cernicharo, Modelling the sulphur chemistry evolution in Orion KL. *Astron. Astrophys.* **567**, A95 (2014).
18. J. C. Laas, P. Caselli, Modeling sulfur depletion in interstellar clouds. *Astron. Astrophys.* **624**, A108 (2019).
19. L. P. Keller *et al.*, Identification of iron sulphide grains in protoplanetary disks. *Nature* **417**, 148–150 (2002).
20. T. H. G. Vidal, V. Wakelam, A new look at sulphur chemistry in hot cores and corinos. *Mon. Not. R. Astron. Soc.* **474**, 5575–5587 (2018).
21. T. H. G. Vidal *et al.*, On the reservoir of sulphur in dark clouds: Chemistry and elemental abundance reconciled. *Mon. Not. R. Astron. Soc.* **469**, 435–447 (2017).
22. C. N. Shingledecker *et al.*, Efficient production of S₀ in interstellar ices: The effects of cosmic-ray-driven radiation chemistry and nondiffusive bulk reactions. *Astrophys. J.* **888**, 52–67 (2020).
23. J. Hatchell, M. A. Thompson, T. J. Millar, G. H. Macdonald, Sulphur chemistry and evolution in hot cores. *Astron. Astrophys.* **338**, 713–722 (1998).
24. S. B. Charnley, Sulfuretted molecules in hot cores. *Astrophys. J.* **481**, 396–405 (1997).
25. D. H. Mordant *et al.*, Primary product channels in the photodissociation of methane at 121.6 nm. *J. Chem. Phys.* **98**, 2054–2065 (1993).
26. M. F. Vernon, "Molecular beam scattering," PhD dissertation, University of California, Berkeley, CA (1983).
27. W. P. Storch, "The reactions of ground and excited state sodium atoms with hydrogen halide molecules," PhD dissertation, University of California, Berkeley, CA (1986).
28. R. D. Levine, *Molecular Reaction Dynamics*, (Cambridge University Press, Cambridge, U.K., 2005).
29. W. B. Miller, S. A. Safron, D. R. Herschbach, Exchange reactions of alkali atoms with alkali halides: A collision complex mechanism. *Discuss. Faraday Soc.* **44**, 108–122 (1967).
30. C. Ochsenfeld, R. I. Kaiser, Y. T. Lee, M. Head-Gordon, Coupled-cluster ab initio investigation of singlet/triplet CH₂S isomers and the reaction of atomic carbon with hydrogen sulfide to HCS/HSC. *J. Chem. Phys.* **110**, 9982–9988 (1999).
31. K. Sato *et al.*, Kinetics and mechanisms of the reactions of CH and CD with H₂S and D₂S. *Chem. Phys.* **242**, 1–10 (1999).
32. S. A. Pope, I. H. Hillier, M. F. Guest, Calculated energetics of rearrangement and fragmentation on the S₀ surface of thioformaldehyde. *J. Chem. Soc. Chem. Commun.* **9**, 623–624 (1984).
33. J. Sarka, A. G. Császár, P. R. Schreiner, Do the mercaptocarbene (H–C–S–H) and selenocarbene (H–C–Se–H) congeners of hydroxycarbene (H–C–O–H) undergo 1,2-h-tunneling? *Collect. Czech. Chem. Commun.* **76**, 645–667 (2011).
34. M. Paranjothy, R. Sun, Y. Zhuang, W. L. Hase, Direct chemical dynamics simulations: Coupling of classical and quasiclassical trajectories with electronic structure theory. *Wiley Interdiscip. Rev. Comput. Mol. Sci.* **3**, 296–316 (2013).
35. S. Pratihari, X. Ma, Z. Homayoon, G. L. Barnes, W. L. Hase, Direct chemical dynamics simulations. *J. Am. Chem. Soc.* **139**, 3570–3590 (2017).

36. A. D. Becke, Density-functional thermochemistry. III. The role of exact exchange. *J. Chem. Phys.* **98**, 5648–5652 (1993).
37. J. Thom, H. Dunning, Gaussian basis sets for use in correlated molecular calculations. I. The atoms boron through neon and hydrogen. *J. Chem. Phys.* **90**, 1007–1023 (1989).
38. P. Pratap *et al.*, A study of the physics and chemistry of TMC-1. *Astrophys. J.* **486**, 862–885 (1997).
39. P. Fleurat-Lessard, J.-C. Rayez, A. Bergeat, J.-C. Loison, Reaction of methylidyne CH($X^2\Pi$) radical with CH₄ and H₂S: Overall rate constant and absolute atomic hydrogen production. *Chem. Phys.* **279**, 87–99 (2002).
40. B. Tercero, J. Cernicharo, J. R. Pardo, J. R. Goicoechea, A line confusion limited millimeter survey of OrionKL I. Sulfur carbon chains. *Astron. Astrophys.* **517**, A96 (2010).
41. D. Prudenzano *et al.*, Accurate millimetre and submillimetre rest frequencies for cis- and trans-dithioformic acid, HCSSH. *Astron. Astrophys.* **612**, A56 (2018).
42. B. A. McGuire *et al.*, Searches for interstellar HCCSH and H₂CCS. *Astrophys. J.* **883**, 201–211 (2019).
43. S. B. Charnley, Chemistry of star-forming cores. *Mol. Grains Space* **312**, 155–159 (1994).
44. T. Lamberts, From interstellar carbon monosulfide to methyl mercaptan: Paths of least resistance. *Astron. Astrophys.* **615**, L2 (2018).
45. T. Yang *et al.*, Gas phase formation of c-SiC₃ molecules in the circumstellar envelope of carbon stars. *Proc. Natl. Acad. Sci. U.S.A.* **116**, 14471–14478 (2019).
46. P. Maksyutenko, F. Zhang, X. Gu, R. I. Kaiser, A crossed molecular beam study on the reaction of methylidyne radicals [CH($X(2)\Pi$)] with acetylene [C(2)H(2)($X(1)\Sigma(g)(+)$)]-competing C(3)H(2) + H and C(3)H + H(2) channels. *Phys. Chem. Chem. Phys.* **13**, 240–252 (2011).
47. D. McElroy *et al.*, The UMIST database for astrochemistry 2012. *Astron. Astrophys.* **550**, A36 (2013).
48. T. Yang *et al.*, Directed gas phase formation of silicon dioxide and implications for the formation of interstellar silicates. *Nat. Commun.* **9**, 774 (2018).